



Article

Expression of Calbindin, a Marker of Gamma-Aminobutyric Acid Neurons, Is Reduced in the Amygdala of Oestrogen Receptor β -Deficient Female Mice

Daniel Kalinowski ^{1,*} , Krystyna Bogus-Nowakowska ¹ , Anna Kozłowska ² and Maciej Równiak ¹

- ¹ Department of Animal Anatomy and Physiology, Faculty of Biology and Biotechnology, University of Warmia and Mazury in Olsztyn, 10-727 Olsztyn, Poland; boguska@uwm.edu.pl (K.B.-N.); mrowniak@uwm.edu.pl (M.R.)
- ² Department of Human Physiology and Pathophysiology, School of Medicine, University of Warmia and Mazury in Olsztyn, 10-082 Olsztyn, Poland; kozłowska.anna@uwm.edu.pl
- * Correspondence: daniel.kalinowski@uwm.edu.pl; Tel./Fax: +48-89-523-4301

Abstract: Oestrogen receptor β (ER β) knock-out female mice display increased anxiety and decreased threshold for synaptic plasticity induction in the basolateral amygdala. This may suggest that the γ -aminobutyric acid (GABA) inhibitory system is altered. Therefore, the immunoreactivity of main GABAergic markers—i.e., calbindin, parvalbumin, calretinin, somatostatin, α 1 subunit-containing GABA_A receptor and vesicular GABA transporter—were compared in the six subregions (LA, BL, BM, ME, CE and CO) of the amygdala of adult female wild-type and ER β knock-out mice using immunohistochemistry and quantitative methods. The influence of ER β knock-out on neuronal loss and glia was also elucidated using pan-neuronal and astrocyte markers. The results show severe neuronal deficits in all main amygdala regions in ER β knock-out mice accompanied by astroglia overexpression only in the medial, basomedial and cortical nuclei and a decrease in calbindin-expressing neurons (CB+) in the amygdala in ER β knock-out mice compared with controls, while other markers of the GABAergic system remain unchanged. Concluding, the lack of ER β led to failure in the structural integrity of the CB+ subpopulation, reducing interneuron firing and resulting in a disinhibitory effect over pyramidal function. This fear-promoting excitatory/inhibitory alteration may lead to the increased anxiety observed in these mice. The impact of neuronal deficits and astroglia overexpression on the amygdala functions remains unknown.



Citation: Kalinowski, D.; Bogus-Nowakowska, K.; Kozłowska, A.; Równiak, M. Expression of Calbindin, a Marker of Gamma-Aminobutyric Acid Neurons, Is Reduced in the Amygdala of Oestrogen Receptor β -Deficient Female Mice. *J. Clin. Med.* **2022**, *11*, 1760. <https://doi.org/10.3390/jcm11071760>

Academic Editors: Lindsay A. Farrer and Seong Soo A. An

Received: 11 February 2022

Accepted: 19 March 2022

Published: 22 March 2022

Publisher's Note: MDPI stays neutral with regard to jurisdictional claims in published maps and institutional affiliations.



Copyright: © 2022 by the authors. Licensee MDPI, Basel, Switzerland. This article is an open access article distributed under the terms and conditions of the Creative Commons Attribution (CC BY) license (<https://creativecommons.org/licenses/by/4.0/>).

Keywords: anxiety disorders; oestrogen receptor β knock-out mice; amygdala; neuronal loss; GABA impairment; immunohistochemistry

1. Introduction

Anxiety disorders are characterised by persistent, overwhelming anxiety and fear, and they affect ~12% of people in a given year and between 5% and 30% over a lifetime [1]. The prevalence of these disorders in women is approximately twice as frequent as in men [2,3]. It has been estimated that in 2017 an estimated 284 million people experienced an anxiety disorder globally, making it the most prevalent mental health disorder [3–6]. Around 63% (179 million) were females, relative to 105 million males [5,7]. Since anxiety disorders affect so many people [8] and often coexist with other psychiatric conditions such as depression, drug addiction and/or personality disorder [3], they constitute a serious social and clinical problem.

The amygdala is essential for fear and anxiety processing [9], and its function is disrupted in anxiety disorders [10]. Moreover, there is also a strong link between altered amygdala processing and depression [11], personality disorder [12] and/or substance abuse [13]. Interestingly, all these emotional disorders occur with different incidence/severity in men vs. women. For example, anxiety disorder and depression are quoted more often in

women [14,15]. In contrast, drug addiction and attention deficit hyperactivity disorder are more common in men [14]. Unfortunately, mechanisms which increase the risk of these diseases in a particular gender are as yet almost unknown.

One of the major factors that may account for sex differences in the incidence/severity of various emotional disorders is altered oestrogen signalling [16,17]. Indeed, a strong association exists between oestrogen and emotional abnormalities in women; e.g., mood swings, anxiety and depression were often linked with low oestrogen levels in women after menopause [18,19]. Oestrogen replacement therapy improves these conditions [20]. Moreover, many reports indicate that the risk of anxiety and depression is greater for perimenopausal women than for premenopausal or postmenopausal women, even after considering various factors such as lifestyle, age, race etc. [21,22]. In addition, behavioural studies in rodents revealed that decreased oestrogen signalling due to oestrogen receptor β (ER β) knock-out leads to increased anxiety [23,24], while ER β agonists usually produce strong anxiolytic effects [25,26]. However, little is known about the mechanisms or sites of actions of oestrogen and neurotransmitter systems involved in these complex modulatory processes. There is currently only evidence that in the adult ER β knock-out mice there are severe cellular deficits in some brain regions, including the medial amygdala, which increase with age [27]. Moreover, these deficits are accompanied by a proliferation of astroglial cells in the limbic structures [27]. There is also evidence reporting a decreased threshold for synaptic plasticity induction in the basolateral amygdala [24], which may suggest that the activity of γ -aminobutyric acid (GABA) inhibitory system is impaired. Interestingly, pharmacological manipulation of GABA type A (GABA_A) receptors in the amygdala of wild-type mice may imitate the effects of ER β knock-out [24]. In fact, decreased GABA signalling in the amygdala might be the beginning of alterations in synaptic plasticity in this region, which result in an anxiety increase in ER β knock-out female mice. Although the expressions of GABA_A receptors and glutamate decarboxylase (GAD) were reported to be unchanged in ER β knock-out mice [24], there are many other possible mechanisms for reducing the inhibitory tone in the amygdala, despite sufficient GABA_A and GAD content [28,29]. One of the possible mechanisms may be, e.g., through serotonergic signalling [30,31] and the 5-hydroxytryptamine 1a receptors [32,33], as the number of these receptors is upregulated in ER β knock-out mice [24].

The amygdala is populated by a large number of γ -aminobutyric acid (GABA)ergic neurons [34], and a large majority of them co-express different calcium-binding proteins and/or neuropeptides [35,36]. These proteins and neuropeptides differentiate GABAergic neurons into discrete subpopulations performing different roles in the inhibitory mechanism of the amygdala. Calbindin (CB), parvalbumin (PV) and calretinin (CR) are usually used to mark these subpopulations in the amygdala [37,38]. In the rat [38] and monkey [39] amygdala, they constitute the bulk of GABAergic neurons. Moreover, axons of parvalbumin-expressing neurons (PV+) target the soma of neighbouring pyramidal cells and cause inhibition [40–42], while axons of neurons utilising CB (CB+) primarily innervate spines and distal dendrites of pyramidal neurons [43]. In contrast, CR-containing neurons (CR+) often target other GABAergic interneurons, as they do in the hippocampus and several cortical regions [44,45], and by inhibiting them disinhibit pyramidal neurons [46,47]. It is worth noting that some CB+ neurons and many PV+ cells are endowed with ER β in wild-type animals, whereas CR+ cells usually contain oestrogen receptors alpha [48,49]. Considering the above, it is very easy to imagine that alterations in the activity of CB+, PV+ and CR+ subpopulations may lead to an alteration in excitatory/inhibitory tone. This may result, for example, in the increased anxiety observed in ER β mutant female mice.

Thus, the aim of the present study was to investigate, for the first time in the amygdala of ER β knock-out female mice, the presence/absence of quantitative alterations among the main markers of the GABAergic system. Such alterations could be the natural basis for inhibitory/excitatory imbalance and increased anxiety in these animals. We chose ER β ^{-/-} females rather than ER β ^{-/-} males, as ER β ^{-/-} females are the best validated animal model of reduced oestrogen signalling and anxiety disorders based on genetic,

behavioural and neurobiological studies [25,50,51]. The following markers were tested: CB, PV and CR, since the cells expressing these proteins constitute the main subsets of the GABAergic population. Additionally, somatostatin (SOM) was also included in the study because it appeared that during the present investigation only the expression of CB+ neurons was reduced in ER β knock-out mice while PV+ and CR+ cells were not affected. Since CB+ neurons in the amygdala include two subsets which are separated and do not overlap—i.e., CB+/PV+ and CB+/SOM+ cells [52]—an additional analysis was performed to clarify whether SOM+ cells are affected. Moreover, vesicular GABA transporter (VGAT) and GABA type A receptor with α 1 subunit (GABA $_A$ α 1) receptors were also tested since alterations in the content of both these proteins also have a huge influence on GABAergic inhibition. VGAT was never investigated in ER β knock-out mice, although GABA type A receptor was tested, but using a quite different method [24]. Finally, the immunoreactivity of neuron-specific nuclear protein (NeuN, pan-neuronal marker) and glial fibrillary acidic protein (GFAP, astrocyte marker) was also investigated in the present study. Severe neuronal deficits and astrocyte overexpression were previously reported in the medial nucleus of the amygdala of the ER β knock-out mice [27], and both of these factors may have an indirect influence on emotional processing [51]. However, the medial nucleus is not strictly linked with anxiety processing [9], whereas the other and relevant amygdala regions were never examined.

2. Materials and Methods

2.1. Animals

Adult female mice—i.e., ER $\beta^{-/-}$ (homozygous B6.129P2-Esr2^{tm1Unc}/J, also known as ER β KO, $n = 6$, aged 6–8 weeks) and ER $\beta^{+/+}$ (C57BL/6J, also known as B6, $n = 6$, aged 6–8 weeks)—were acquired from the Jackson Laboratory (Bar Harbor, ME, USA) and transported to the animal house at the Faculty of Veterinary Medicine of the University of Warmia and Mazury (Olsztyn, Poland). Both ER $\beta^{-/-}$ and ER $\beta^{+/+}$ mice were acclimatised one week and housed in a temperature-controlled (21 ± 1 °C) and ventilated (12–20 air exchanges/h) animal room which maintained a 12/12 h light/dark cycle (lights on from 6:00 to 18:00). They were kept separately in sanitised polypropylene cages in groups of two/three to avoid stress from isolation and had free access to a standard mice grain mixture (devoid of phytoestrogens; LabDiet[®] JL Rat and Mouse/Auto 6F 5K52) and tap water ad libitum. Animal care and handling were in strict accordance with the European Union Directive for animal experiments (2010/63/EU) and the 3Rs principle (Replacement, Reduction and Refinement); thus, all animals used were registered, and the staff was adequately educated and trained (Certificate No 1267/2015). According to the Act of 15 January 2015 on the protection of animals used for scientific and educational purpose (adopted in Poland), if the only activity is killing an animal for collecting tissues or organs, it is not considered a procedure, so ethics committee approval is not required. All efforts were made to minimize animal suffering and to use the minimum number of animals necessary to generate reliable scientific data.

2.2. Tissue Preparation

Following a two-week habituation phase, all ER $\beta^{-/-}$ and ER $\beta^{+/+}$ mice were subjected to the same laboratory procedures. First, the oestrous cycle was monitored, and the stage of the oestrous cycle was determined directly from vaginal smears. Cycle monitoring is necessary as both ER $\beta^{-/-}$ and ER $\beta^{+/+}$ show normative patterns of steroid hormone levels [52], and these steroids fluctuate during the oestrous cycle, which may affect the anxiety behaviour, as was described by Dombret [53]. Therefore, to avoid the oestrogen-induced anxiolytic effect, all mice were anaesthetised in metestrus, as this phase is characterized by a low oestrogen level [54]. The mice were then deeply anaesthetised with an intraperitoneal injection of pentobarbital (Morbital, Biowet, Poland; 2 mL/kg) according to the guidelines of the Humane Society Veterinary Medical Association, and after cessation of breathing, immediately perfused transcardially with saline (0.9%) followed by 4% paraformaldehyde

(PFA; pH 7.4; 1040051000, Merck, Germany) in phosphate-buffered saline (PBS; P5493, Sigma-Aldrich, Darmstadt, Germany). After perfusion, the brains were dissected and post-fixed by immersion in 4% PFA overnight, washed three times in 0.1 M phosphate buffer (pH = 7.4, 4 °C) and then cryoprotected for 3–5 days in graded solutions (10%, 20% and 30%) of sucrose (363-117720907, ALCHEM, Poland) in 1×PBS at 4 °C. Finally, the brains were frozen and then sectioned in the coronal plane at a thickness of 10 µm with the use of a cryostat (HM525 Zeiss, Germany). The sections were mounted on object slides and stored at −80 °C until further processing.

2.3. Immunohistochemistry

Selected amygdala sections from ERβ^{−/−} and ERβ^{+/+} mice were stained using two immunohistochemical methods: immunoperoxidase labelling with 3,3-diaminobenzidine (DAB) as a substrate-chromogen and immunofluorescence. All staining steps were performed at room temperature in humid chambers (Immuno Slide Staining Trays, R64001-E, Pyramid Innovation Ltd., Polegate, UK).

DAB staining. To visualize the location and borders of the individual amygdala regions with the use of NeuN (pan-neuronal marker) and populations of neurons expressing CB, PV or CR in these regions, selected brain sections were labelled using the DAB technique (Table 1) described in detail in the authors' previous papers [55]. Briefly, these sections, after triple washing in PBS, were pre-incubated for 30 min in 0.3% H₂O₂ diluted in 99.85% methanol and then for 60 min with a solution of 10% normal donkey serum (diluted in PBS). The sections were then incubated overnight with a solution of primary antibodies, which were diluted in PBS with 1% normal donkey serum and Triton X-100 (0.3–0.5%). The next day, the sections were triple-washed in PBS, treated with the solution of peroxidase-conjugated secondary antibodies (Imm-PRESS Reagent) for one hour, and finally incubated with a 3% DAB solution (Table 1). In the final step, sections were rinsed with water, dehydrated using a series of graded alcohol dilutions (POCH, Poland), cleaned in xylene and mounted in DPX (DPX Mountain for histology; 44581, Sigma-Aldrich, Germany).

Table 1. Specification of reagents.

Antigen	Code	Clonality	Host Species	Dilution	Supplier	Location
Primary antibodies						
NeuN	ABN78	polyclonal	Rabbit	1:1000	Millipore	Temecula, CA, USA
CB	CB-38	polyclonal	Rabbit	1:4000	SWANT	Bellinzona, Switzerland
PV	PV27	polyclonal	Rabbit	1:1000	SWANT	Bellinzona, Switzerland
CR	7697	polyclonal	Rabbit	1:1000	SWANT	Bellinzona, Switzerland
SOM	MAB354	monoclonal	Rat	1:1000	Millipore	Temecula, CA, USA
GABA _A α1	AB33299	polyclonal	Rabbit	1:2000	Abcam	Cambridge, UK
VGAT	AB5062P	polyclonal	Rabbit	1:3000	Millipore	Temecula, CA, USA
GFAP	G9269	polyclonal	Rabbit	1:200	Millipore	Temecula, CA, USA
Secondary antibodies						
ImmPRESS HRP Universal Antibody (anti-rabbit Ig, Peroxidase)				1:1	Vector Laboratories	Burlingame, CA, USA
ALEXA Fluor 555	A-31572	polyclonal	Donkey anti-rabbit	1:1000	Thermo Fisher	Rockford, IL, USA
CY3	712-165-153	polyclonal	Donkey anti-rat	1:1000	Jackson ImmunoResearch Laboratories	West Grove, PA, USA
Other reagents						
3,3-diaminobenzidine substrate chromogen				3%	Dako Cytomation	Glostrup, Denmark

Immunofluorescence. To visualize SOM, GABA_Aα1, VGAT and GFAP signal in the amygdala, selected sections in both ERβ^{-/-} and ERβ^{+/+} mice were subjected to routine immunofluorescence, with full details in Równiak's work [43]. Briefly, the sections were triple-washed with PBS and then incubated for one hour with a blocking buffer composed of 0.1 M PBS, 10% normal donkey serum, 0.1% bovine serum albumin, 0.05% thimerosal and 1% Tween. After this, the sections were triple-washed in PBS and then incubated overnight with a solution of primary antibodies directed to SOM, GABA_Aα1, VGAT and GFAP (Table 1). The antibodies were diluted in a blocking buffer. Finally, the sections were rinsed in PBS, incubated for one hour with the secondary antibodies' solution (Table 1), mounted with carbonate-buffered glycerol (pH 8.6) and coverslipped.

2.4. Controls

The primary antibodies used in the study were carefully chosen. The specificity of the primary antisera used in this study was shown by various researchers using these products in previous immunohistochemical studies [27,56–60]. The rabbit antibody against neuron-specific nuclear protein NeuN (ABN78) was positively validated by the manufacturer using Western blotting in mouse brain extracts, showing bands ~48/42 kDa. Moreover, product descriptions of the rabbit antibodies against calcium-binding proteins, such as anti-calbindin (CB-38), anti-parvalbumin (PV27) and anti-calretinin (7697), demonstrate data with immunoblots carried out using the mouse brain extracts, which show specific bands for these proteins at 28 kDa, 12 kDa and 29 kDa, respectively. These datasheets also demonstrate a lack of any immunostaining in sections taken from the brains of CB, PV or CR knock-out mice by using the mentioned antibodies. Finally, the rabbit antibodies against GABA_Aα1 (ab33299) and VGAT (ab5062P) were successfully validated by Western blots in mouse brain homogenates [61,62]. The specificity of the secondary antibodies was evaluated by omitting or replacing primary antibodies with non-immune sera or PBS. The absence of any immunosignal demonstrated specificity. Finally, to check whether the staining was specific, it was always analysed in the blue (UV), green (488 nm) and red (555 nm) fluorescent channels.

2.5. Counts and Measurements

To quantify the density of NeuN+, CB+, PV+, CR+ or SOM+ neurons in the studied amygdala nuclei, the stained sections were examined using an Olympus BX51 microscope (Olympus GmbH, Germany) with a digital camera (CC-12, Soft Imaging System, Münster, Germany) and Cell-F software (Olympus, Hamburg, Germany). The following amygdala nuclei were tested: lateral (LA), basolateral (BL), basomedial (BM), medial (ME), central (CE) and cortical (CO). It is necessary to note that the delineation pattern of various amygdaloid nuclei and nomenclature for the amygdala used in the present study were adopted without modifications from the mouse brain atlas of Paxinos and Franklin [63]. For each nucleus in each animal of both ERβ^{-/-} and ERβ^{+/+} mice, NeuN+, CB+, PV+, CR+ or SOM+ cells were counted on fifteen evenly spaced sections (per antigen) arranged from the rostral (bregma = -1.06) to the caudal extent (bregma = -2.30) of the amygdala [63]. The distance between sections was 70–80 μm. Counting on the single strip was always done with a 40× lens and with the use of 347.6 μm × 260.7 μm regions (test frames). These frames were always distributed to ensure coverage of the full area of the analysed nucleus. The number of test frames per nucleus was diversified: LA: 1–4, BL: 2–6, BM: 2–3, CO: 1–2, ME: 4–6 and CE: 2–3. The counts calculated within the single test frame were averaged, and they had to always be recalculated to value a corresponding to the area of 0.04 mm² or 0.04 mm³. The mean values from the test frames covering the particular nucleus on the section were averaged. To calculate neuron density in the particular nucleus in the subject, the results from individual strips were averaged. In the last step, values from the individual nuclei were also averaged in each mice group and saved in the format: mean ± standard deviation (SD).

To evaluate the volume density of GABA_Aα1 and VGAT immunoreactive (IR) elements in the amygdala nuclei, the immunofluorescence-stained sections were analysed according to the automated line scan analysis described and validated by Sathyanesan et al. [64]. Briefly, images acquired with Olympus BX51 microscope were feature-extracted using a Hessian-based filter included in the plugin called FeatureJ [65] for NIH ImageJ software (version 1.53e). These images were then subjected to line scan profile analysis using five lines oriented horizontally (parallel scans) and five lines oriented vertically (perpendicular scans). In the next step, the line scans were baseline-adjusted and processed with the algorithm for peak-detection. Estimation of baseline depends on how peaks (signal) are distinguishable from the background. To evaluate the background value for the line scans, these scans were also always drawn from several immune-negative places. The mean was then calculated from these measurements and constituted the final background value for the single section (threshold). Such a threshold is required for a peak-detection algorithm. Finally, the volume density of GABA_Aα1 and VGAT was calculated using the formula presented by Sathyanesan [64]. The same images were also subjected to signal intensity evaluation using measure analyses by integrated density (IntDen) in NIH ImageJ software. All the measurements in all nuclei in the subjects were determined on ten evenly spaced sections (per antigen) on images covering the whole cross-section area of the nuclei.

The GFAP immunoreactivity was analysed on five evenly spaced sections without cell counting, since the difference in immunoreactive signal was so evident in the selected amygdala regions between ERβ^{-/-} and ERβ^{+/+} mice that cell counts were not necessary.

All measurements were determined by the first author on coded slides, and then the analyses were repeated by two independent researchers, all being blind to the parameters of the studied tissue (knock-out mice vs. wild-type mice). The comparisons of results revealed high inter-rater reliability (Pearson R = 0.88).

2.6. Statistics

The mixed model was used for investigations. The parametric method was used throughout the analysis. Briefly, all calculations were performed using Statistica 13.3 (TIBCO Software Inc., Palo Alto, CA, USA). The differences between two independent groups (knock-out mice vs. wild-type mice) in statistical tests were calculated assuming that the statistical significance $\alpha = 0.05$, and statistical power $(1 - \beta)$ was equal to 0.95, and the allocation ratio was 1:1. Because the sample size of the knock-out mice group and the wild-type mice group was six in each subject, fifteen or ten sections were analysed, and the total number per group was ninety or sixty, respectively. The data from neurohistological research were averaged and examined for normal distribution by Shapiro–Wilk tests. The statistical graphs were produced by GraphPad Prism 6 software (GraphPad Software, La Jolla, CA, USA). The data are expressed as a box-and-whisker plots with the “box” depicting the median and 25th and 75th quartiles and “whiskers” showing the 5th and 95th percentile ($n = 6$). An independent-sample t-test was used to determine the differences between groups. The examined homogeneity of variance was used, and correction of Cochran’s Q test was then applied. The level of significance was set at $p \leq 0.05$.

3. Results

The results of the present study demonstrate severe neuronal deficits in all main amygdala regions in ERβ knock-out mice, accompanied by astroglia overexpression only in the medial, basomedial and cortical nuclei. Additionally, the density of CB+ neurons in the amygdala is significantly reduced in ERβ knock-out mice compared with matched controls, while the expressions of other markers of the GABAergic system such as PV, CR, SOM, GABA_Aα1 and VGAT are not affected by ERβ deficiency.

3.1. Neuronal Deficits in the Amygdala of ERβ^{-/-} Mice

DAB staining with the use of an anti-NeuN antibody (pan-neuronal marker) revealed a significant neuronal deficit in all amygdala nuclei of ERβ^{-/-} mice when compared with

ERβ^{+/+} (Figures 1A and 2, Table 2). In the basolateral amygdala, the neuronal deficit was in a range of 16–19%. In the medial amygdala, the neuronal deficit was the most pronounced (~22%), while it was the smallest in the cortical and central amygdala (~14%).

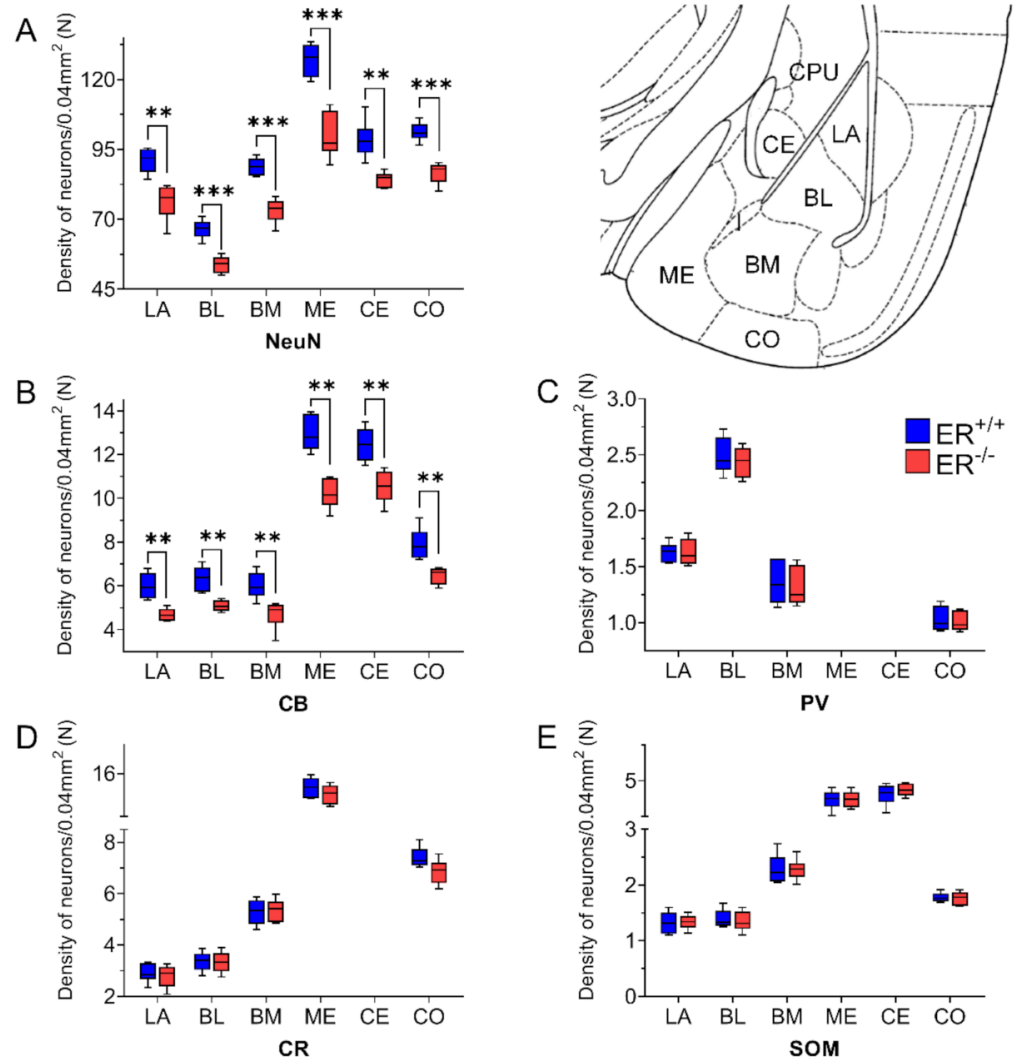


Figure 1. The density of neuron-specific nuclear protein (NeuN)-, calbindin (CB)-, parvalbumin (PV)-, calretinin (CR)- and somatostatin (SOM)-expressing neurons in the amygdala of wild-type (ERβ^{+/+}) and ERβ and knock-out (ERβ^{-/-}) mice. Note that the density of cells expressing NeuN (A) and CB (B) is significantly reduced in ERβ knock-out mice when compared with wild-type mice, while values for PV (C), CR (D) and SOM (E) did not differ in both ERβ^{-/-} and ERβ^{+/+} mice. Data are expressed as a box-and-whisker plots, with the “box” depicting the median and 25th and 75th quartiles and “whiskers” showing 5th and 95th percentile (*n* = 6). ** (*p* ≤ 0.01) and *** (*p* ≤ 0.001) indicate statistically significant differences between wild-type and ERβ knock-out mice. LA—lateral nucleus, BL—basolateral nucleus, BM—basomedial nucleus, ME—medial nucleus, CE—central nucleus, CO—cortical nucleus, I—intercalated nucleus, CPU—caudate-putamen complex.

Table 2. Statistical analysis of studied markers between ERβ^{+/+} and ERβ^{-/-} mice in the amygdala.

	LA		BL		BM		ME		CE		CO	
	<i>t</i>	<i>p</i>	<i>t</i>	<i>p</i>	<i>t</i>	<i>p</i>	<i>t</i>	<i>p</i>	<i>t</i>	<i>p</i>	<i>t</i>	<i>p</i>
NeuN	t _{8.88} = 4.77	0.001057	t _{9.70} = 6.88	0.000051	t _{9.02} = 7.25	0.000048	t _{8.98} = 6.74	0.000085	t _{9.78} = 7.05	0.000039	t _{6.66} = 4.86	0.002112
CB	t _{7.27} = 4.74	0.001913	t _{7.27} = 4.74	0.002045	t _{9.55} = 4.16	0.004259	t _{9.58} = 6.33	0.001030	t _{9.99} = 4.46	0.001229	t _{7.80} = 4.40	0.002435
PV	t ₁₀ = 0.054	0.9581	t ₁₀ = 0.62	0.5482	t ₁₀ = 0.48	0.6642	–	–	–	–	t ₁₀ = 0.46	0.6581
CR	t ₁₀ = 0.53	0.6113	t ₁₀ = 0.16	0.8787	t ₁₀ = -0.24	0.8119	t ₁₀ = 1.24	0.2426	–	–	t ₁₀ = 2.13	0.0594
SOM	t ₁₀ = -0.22	0.8274	t ₁₀ = 0.08	0.9344	t ₁₀ = -0.26	0.8036	t ₁₀ = 0.17	0.8662	t ₁₀ = 0.63	0.5441	t ₁₀ = 0.16	0.8732
GABA _A α1	t ₁₀ = 0.35	0.7337	t ₁₀ = 0.11	0.9178	t ₁₀ = -0.62	0.5478	t ₁₀ = 0.08	0.9357	t ₁₀ = -0.19	0.8513	t ₁₀ = 0.11	0.9106
Intensity of GABA _A α1	t ₁₀ = 0.94	0.3674	t ₁₀ = 0.97	0.3536	t ₁₀ = 1.24	0.2445	t ₁₀ = -0.82	0.4334	t ₁₀ = -0.85	0.4133	t ₁₀ = -0.08	0.9379
VGAT	t ₁₀ = -0.22	0.8274	t ₁₀ = 0.08	0.9344	t ₁₀ = -0.26	0.8036	t ₁₀ = 0.17	0.8662	t ₁₀ = 0.63	<i>p</i> = 0.5441	t ₁₀ = 0.16	0.8732
Intensity of GABA _A α1	t ₁₀ = -0.57	0.5829	t ₁₀ = -1.00	0.3432	t ₁₀ = -0.29	0.7796	t ₁₀ = -0.31	0.7607	t ₁₀ = 0.19	<i>p</i> = 0.8495	t ₁₀ = 1.07	0.3091

Lack of immunoreactive structures was marked as a dash.

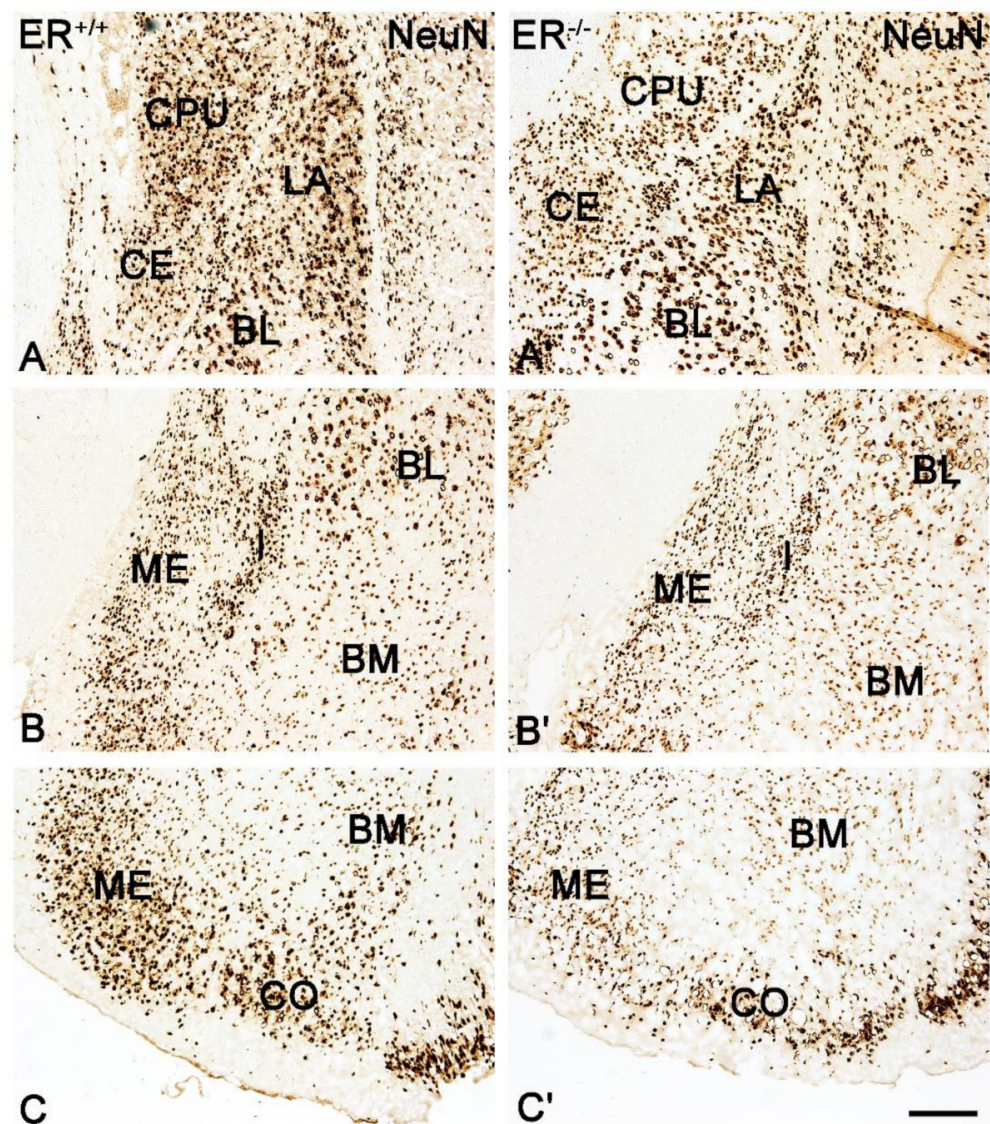


Figure 2. Brightfield photomicrographs illustrating the immunoreactivity patterns of neuron-specific nuclear protein (NeuN) in the amygdala of the wild-type ($ER\beta^{+/+}$, (A–C)) and $ER\beta$ knock-out ($ER\beta^{-/-}$, (A',C')) mice. (A,A'): The lateral (LA), basolateral (BL), central (CE) nuclei and caudate-putamen complex (CPU). (B,B'): The medial (ME), intercalated (I), basolateral (BL) and basomedial (BM) nuclei. (C,C'): The medial (ME), basomedial (BM) and cortical (CO) nuclei. Note the reduced density of NeuN+ neurons in the $ER\beta$ knock-out (A'–C') subjects. Scale bar = 200 μ m.

3.2. Calcium-Binding Proteins in the Amygdala of $ER\beta^{-/-}$ Mice

Both the distribution and characteristics of CB+, PV+ and CR+ staining were comparable in $ER\beta^{-/-}$ and $ER\beta^{+/+}$ mice, and they closely matched earlier results from the adult rat brain [37]. The only exception was the CE in CR+ preparations which, similar to the guinea pig amygdala [55], had strongly stained neuropil but only a few immunopositive cells. As in other animals, CB+, PV+ and CR+ immunoreactivity in mice was mostly observed in perikarya and dendrites, but puncta were also present (Figures 3–6). It is worth noting that in both $ER\beta^{-/-}$ and $ER\beta^{+/+}$ the distribution pattern for CB+, PV+ and CR+ in each nucleus gradually changed along a rostral to caudal gradient. However, this gradient was not observed among other markers studied. Despite the overall similarity in the immunoreactivity pattern in $ER\beta^{-/-}$ and wild-type mice, the density of CB+ neurons was substantially decreased in all amygdala regions of $ER\beta^{-/-}$ mice (Figures 1B and 3, Table 2). In the basolateral and medial regions of the amygdala, the CB+ decrease was in the range of

19–22%. In the central and cortical regions of the amygdala, this decrease was also present, but it was less pronounced (15–18%). To the contrary, the density of PV+ and CR+ neurons was not affected due to ER β deficiency (Figure 1C,D, Figures 4 and 5, Table 2).

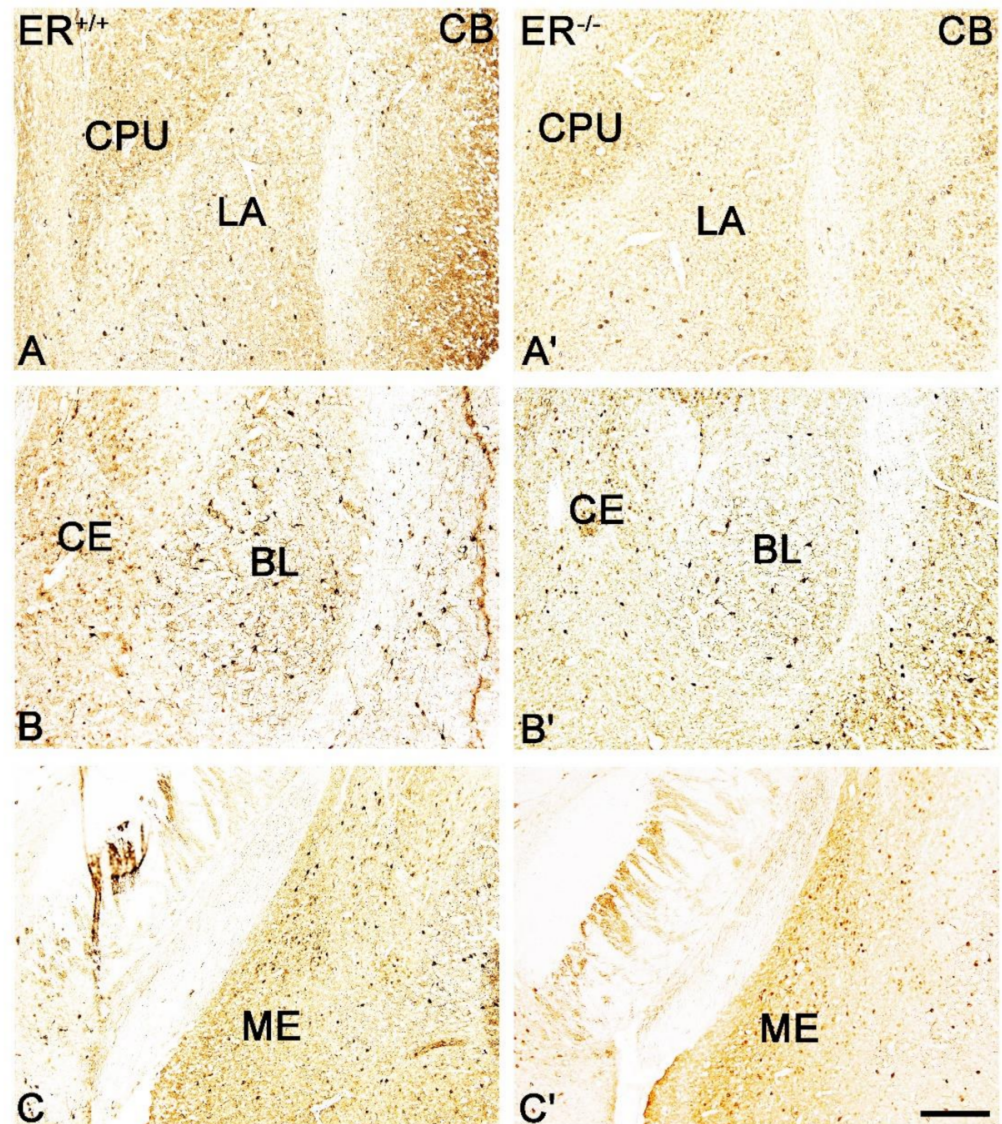


Figure 3. Brightfield photomicrographs highlighting the immunoreactivity patterns of calbindin (CB) in the amygdala of the wild-type (ER $\beta^{+/+}$, (A–C)) and ER β knock-out (ER $\beta^{-/-}$, (A'–C')) mice. (A,A'): The lateral (LA) nuclei and caudate-putamen complex (CPU). (B,B'): The basolateral (BL) and central (CE) nuclei. (C,C'): The medial (ME) nucleus. Note the reduced density of CB+ neurons in the ER β knock-out (A'–C') subjects. Scale bar = 200 μ m.

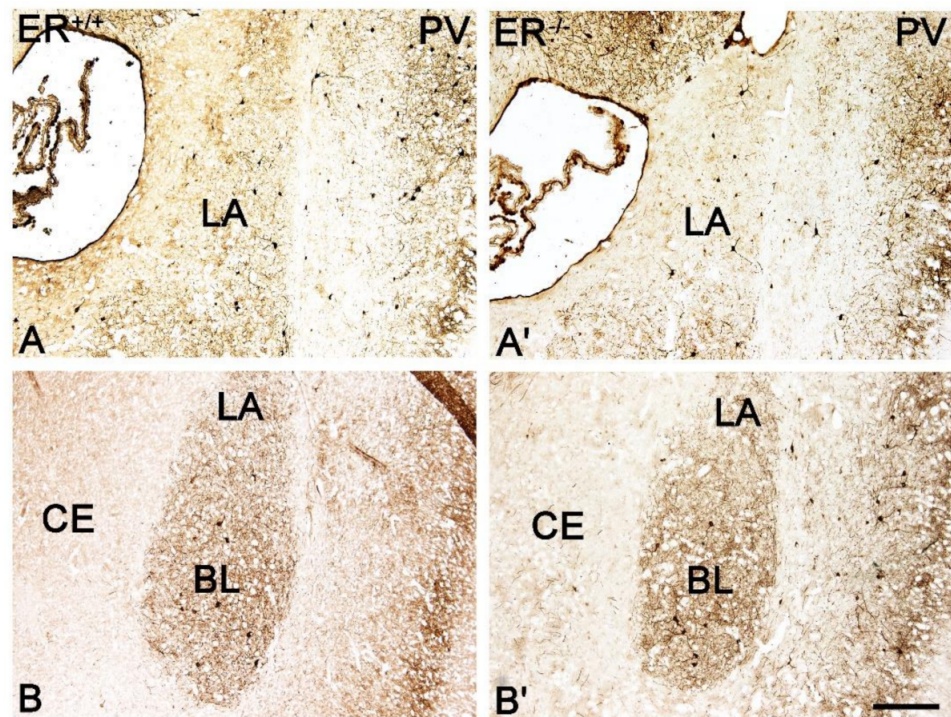


Figure 4. Brightfield photomicrographs highlighting the immunoreactivity patterns of parvalbumin (PV) in the amygdala of the wild-type ($ER\beta^{+/+}$, (A,B)) and $ER\beta$ knock-out ($ER\beta^{-/-}$, (A',B')) mice. (A,A'): The lateral (LA) nucleus. (B,B'): The lateral (LA), basolateral (BL) and central (CE) nuclei. Note similar density of PV+ neurons in the wild-type (A,B) and $ER\beta$ knock-out (A',B') subjects. Scale bar = 200 μ m.

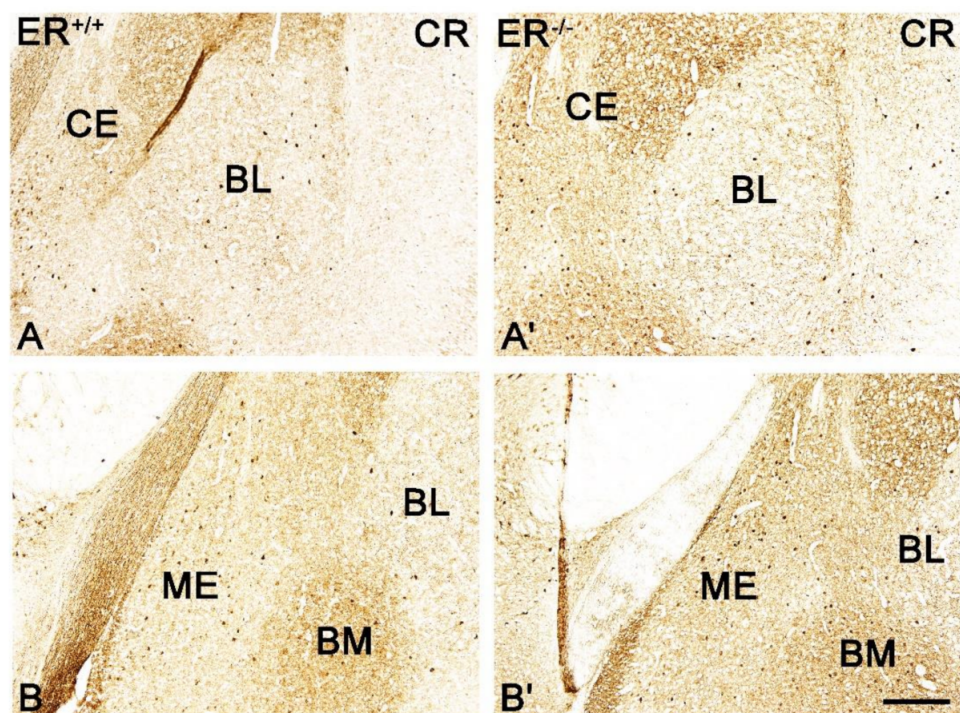


Figure 5. Brightfield photomicrographs highlighting the immunoreactivity patterns of calretinin (CR) in the amygdala of the wild-type ($ER\beta^{+/+}$, (A,B)) and $ER\beta$ knock-out ($ER\beta^{-/-}$, (A',B')) mice. (A,A'): The basolateral (BL) and central (CE) nuclei. (B,B'): The medial (ME), basolateral (BL) and basomedial (BM) nucleus. Note similar density of CR+ neurons in the wild-type (A,B) and $ER\beta$ knock-out (A',B') subjects. Scale bar = 200 μ m.

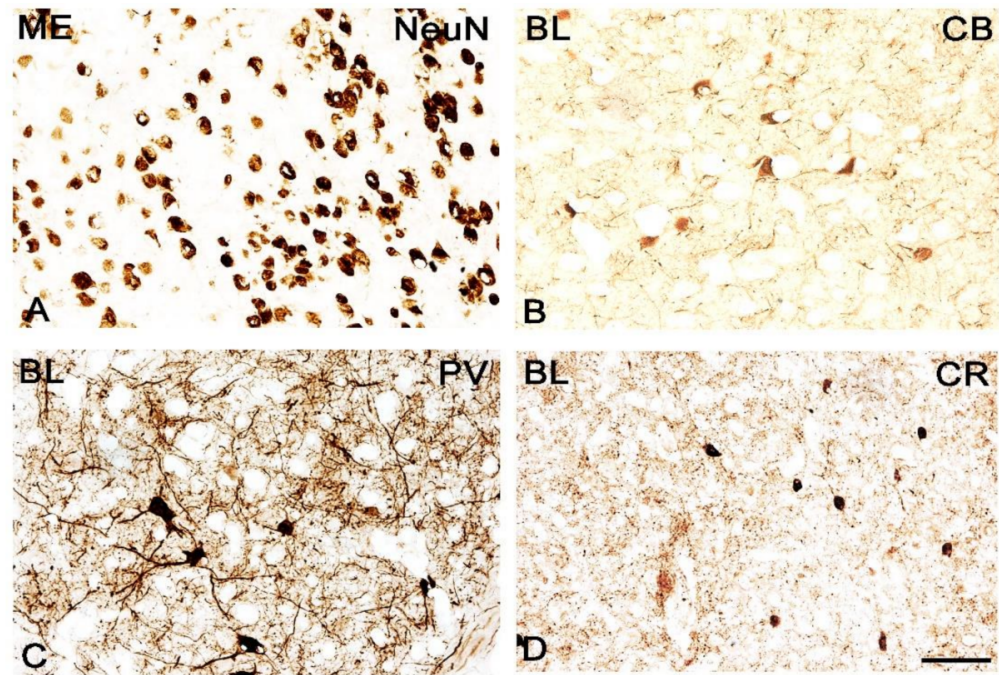


Figure 6. Brightfield photomicrographs illustrating the immunoreactivity of cellular structures of neuron-specific nuclear protein (NeuN, (A)), calbindin (CB, (B)), parvalbumin (PV, (C)) and calretinin (CR, (D)) of wild-type in the mice amygdala. (A): The medial (ME) and (B–D): The basolateral (BL). Scale bar = 50 μ m.

3.3. Somatostatin in the Amygdala of $ER\beta^{-/-}$ Mice

The distribution and characteristics of somatostatin immunoreactivity were very similar in both $ER\beta^{-/-}$ and $ER\beta^{+/+}$ mice and did not differ from results reported previously within the adult mouse and rat brain [50]. Somatostatin staining was present in all amygdala nuclei, and it consisted mostly of somata and dendrites, although immunoreactive puncta were also present (Figure 7). Staining similarity was confirmed by a morphometric analysis since the density of SOM+ neurons was unchanged in all amygdala regions in $ER\beta^{-/-}$ mice when compared with $ER\beta^{+/+}$ mice (Figures 1E and 7, Table 2).

3.4. GABA Type A Receptor with $\alpha 1$ Subunit in the Amygdala of $ER\beta^{-/-}$ Mice

The distribution and characteristics of GABA_A $\alpha 1$ + immunoreactivity were quite similar in both $ER\beta^{-/-}$ and $ER\beta^{+/+}$ mice, and they closely matched previous observations in the rodent amygdala [49,66–68]. GABA_A $\alpha 1$ + staining was usually observed in dendrites, although positive somata and puncta were also frequently present (Figure 9). The immunoreactive elements in the amygdala were fairly uniformly distributed, except BL with the highest expression and CE with the lowest content (Figure 8A,C and Figure 9). Moreover, the cells were the most frequent in BL, whereas the most immunoreactive neuropil was present in the dorsal part of LA. As a large part of GABA_A $\alpha 1$ immunoreactivity was actually present in dendrites, immunoreactive puncta densitometric analysis was performed. This analysis revealed a lack of any significant differences in the volume density and signal intensity of GABA_A $\alpha 1$ + elements between $ER\beta^{-/-}$ and wild-type mice (Figure 8A,C, Table 2).

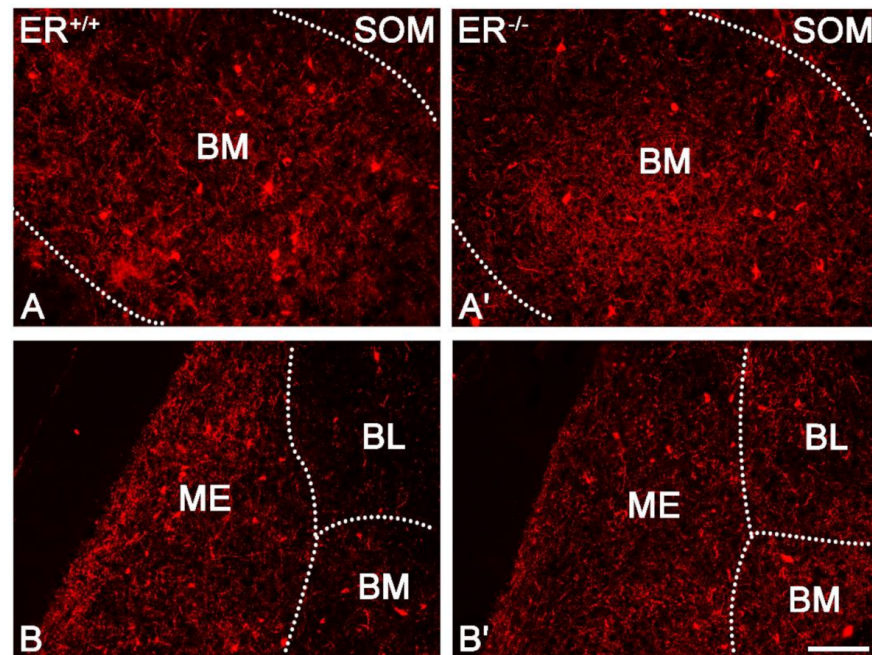


Figure 7. Representative colour photomicrographs illustrating the staining pattern of somatostatin (SOM) in the amygdala of wild-type ($ER\beta^{+/+}$, (A,B)) and $ER\beta$ knock-out ($ER\beta^{-/-}$, (A',B')) mice. (A,A'): The basomedial (BM) nucleus. (B,B'): The medial (ME), basolateral (BL) and basomedial (BM) nucleus. Note similar density of SOM+ neurons in the wild-type (A,B) and $ER\beta$ knock-out (A',B') subjects. Scale bar = 100 μ m.

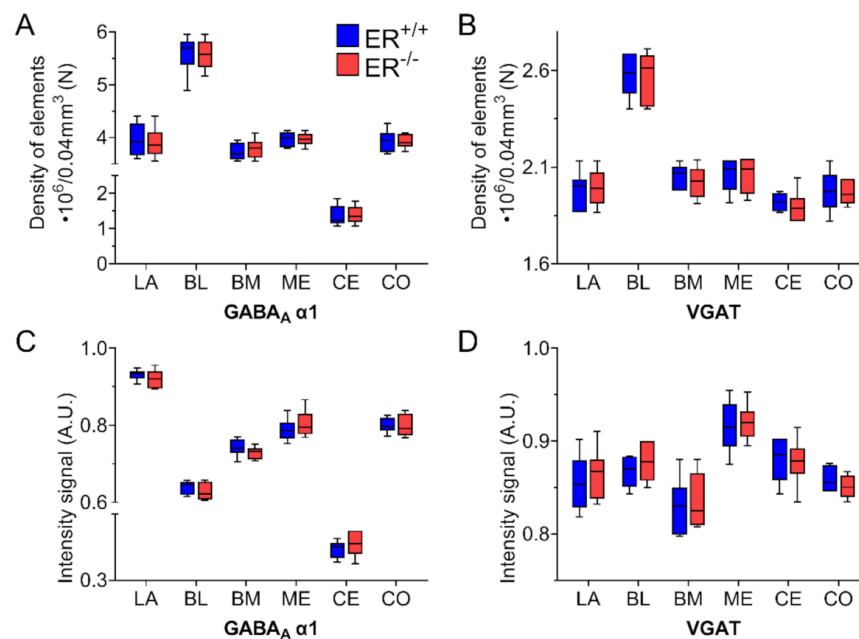


Figure 8. The volume density (elements) and signal intensity of GABA type A receptor with $\alpha 1$ subunit ($GABA_A \alpha 1$) and vesicular GABA transporter (VGAT) in the amygdala of wild-type ($ER\beta^{+/+}$) and $ER\beta$ knock-out ($ER\beta^{-/-}$) mice. Note that the volume density (elements) of $GABA_A \alpha 1$ (A) and VGAT (B) is similar in wild-type and $ER\beta$ knock-out mice. Note also that the signal intensity of $GABA_A \alpha 1$ (C) and VGAT (D) is also similar in both $ER\beta^{-/-}$ and $ER\beta^{+/+}$ mice. Data are expressed as a box-and-whisker plots, with the “box” depicting the median and 25th and 75th quartiles, and “whiskers” showing 5th and 95th percentile ($n = 6$). LA—lateral nucleus, BL—basolateral nucleus, BM—basomedial nucleus, ME—medial nucleus, CE—central nucleus, CO—cortical nucleus.

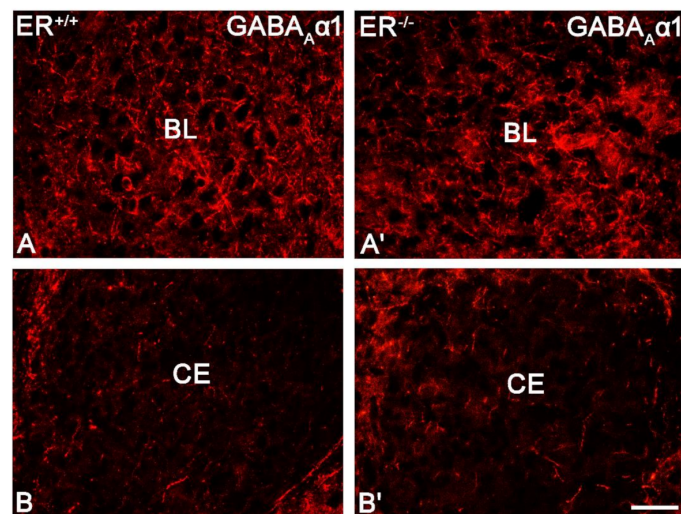


Figure 9. Representative colour photomicrographs illustrating the staining pattern of GABA type A receptor with $\alpha 1$ subunit ($GABA_A\alpha 1$) in the amygdala of wild-type ($ER\beta^{+/+}$, (A,B)) and $ER\beta$ knock-out ($ER\beta^{-/-}$, (A',B')) mice. (A,A'): The basolateral (BL) nucleus. (B,B'): The central (CE) nucleus. Note similar density (elements) and signal intensity of $GABA_A\alpha 1$ in the wild-type (A,B) and $ER\beta$ knock-out (A',B') subjects. IR elements—immunoreactive structures which include somata, fibres and puncta. Scale bar = 50 μm .

3.5. Vesicular GABA Transporter in the Amygdala of $ER\beta^{-/-}$ Mice

The VGAT+ immunoreactivity pattern did not differ between $ER\beta^{-/-}$ and $ER\beta^{+/+}$ mice, and it generally consisted of immunoreactive puncta, although fibres were also present (Figure 10). The distribution of immunoreactive elements was rather homogenous and high in the whole amygdala except the BL with the highest content, although the signal intensity in the medial amygdala was slightly higher than in the basolateral region of the amygdala (Figure 8B,D and Figure 10). Densitometric comparisons did not show important differences in the volume density and signal intensity (Table 2).

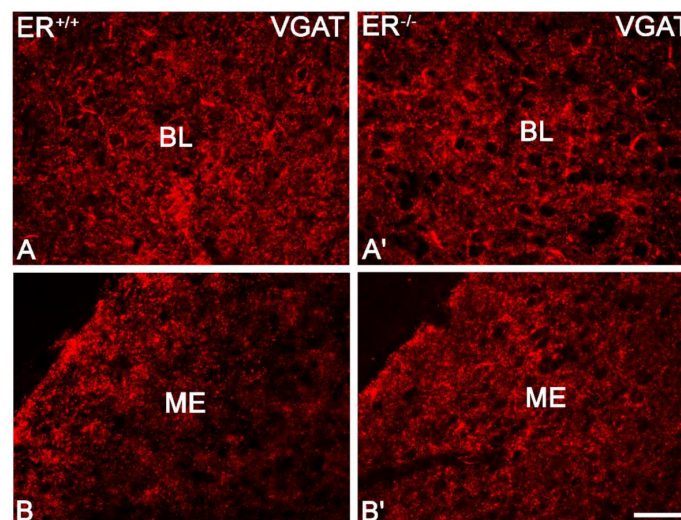


Figure 10. Representative colour photomicrographs illustrating the staining pattern of vesicular GABA transporter (VGAT) in the amygdala of wild-type ($ER\beta^{+/+}$, (A,B)) and $ER\beta$ knock-out ($ER\beta^{-/-}$, (A',B')) mice. (A,A'): The basolateral (BL) nucleus. (B,B'): The medial (ME) nucleus. Note similar density (elements) and signal intensity of VGAT in the wild-type (A,B) and $ER\beta$ knock-out (A',B') subjects. IR elements—immunoreactive structures which include somata, fibres and puncta. Scale bar = 50 μm .

3.6. Overexpression of Glial Fibrillary Acidic Protein in the Amygdala of $ER\beta^{-/-}$ Mice

GFAP-stained samples revealed significant overexpression of GFAP (astrocytes) in the $ER\beta$ knock-out mice compared with wild-type in selected amygdala nuclei, such as ME, BM and CO. However, the other regions such as LA, BL and CE were not affected in these mice (Figure 11).

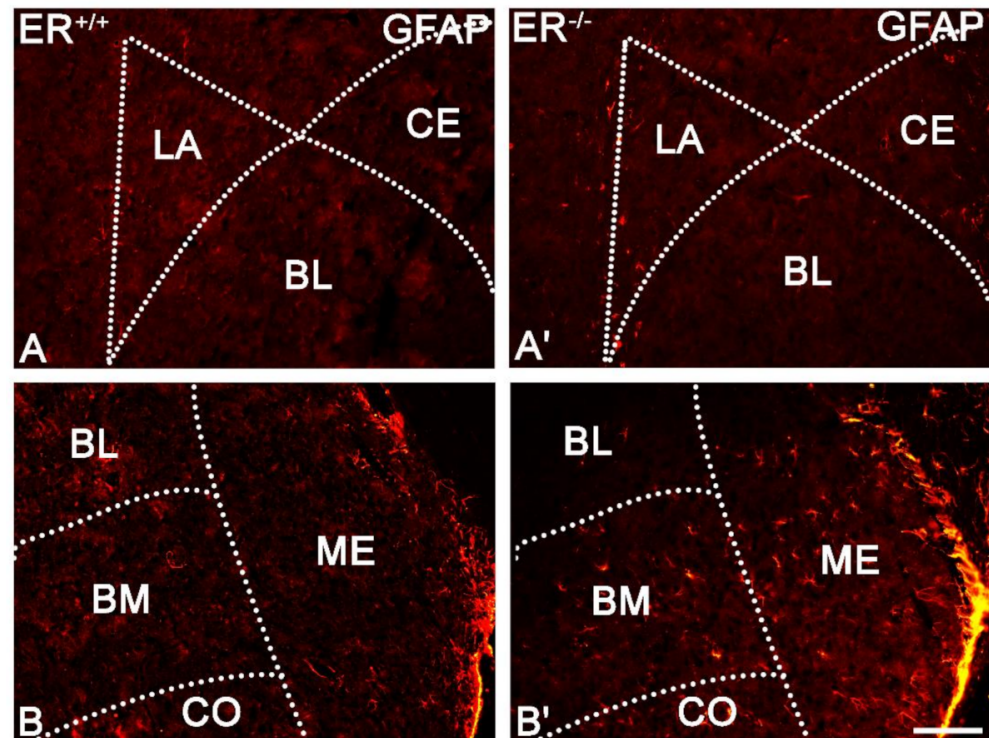


Figure 11. Representative colour photomicrographs illustrating the staining pattern of glial fibrillary acidic protein (GFAP) in the amygdala of wild-type ($ER\beta^{+/+}$, (A,B)) and $ER\beta$ knock-out ($ER\beta^{-/-}$, (A',B')) mice. (A,A'): The lateral (LA), basolateral (BL) and central (CE) nuclei. (B,B'): The basolateral (BL), basomedial (BM), cortical (CO) and medial (ME) nuclei. Note increased content of GFAP cells in the BM, CO and ME of $ER\beta$ knock-out subjects (B'). Note also the lack of such staining in the LA, BL and CE (A'). Scale bar = 100 μ m.

4. Discussion

The results provide evidence of severe neuronal deficits in all main amygdala regions accompanied by astroglia overexpression in ME, BM and CO and show that the density of CB+ neurons, the largest subset of GABA+ neurons [37], in the amygdala of $ER\beta$ knock-out female mice is significantly reduced in comparison with $ER\beta^{+/+}$. In contrast, the density of PV+, CR+ and SOM+ neurons, as well as GABA $_A$ α 1 and VGAT content, are unchanged in these mice. These results provide evidence that the lack of $ER\beta$ in mutant female mice affects the expression of CB in the GABAergic amygdala, causing a reduction in interneuron firing [69,70] and an eventual disinhibitory effect on pyramidal function [71]. This fear-promoting excitatory/inhibitory alteration may result in increased anxiety in these mice. The impact of neuronal deficits and astroglia overexpression on the amygdala functions is currently unknown.

The study demonstrated that in the amygdala of $ER\beta$ knock-out female mice, the density of CB+ neurons is significantly decreased relative to $ER\beta^{+/+}$ mice, while PV+ and CR+ cells remain unaffected. This coincides well with the fact that the CB reduction modifies fear, anxiety and social behaviours in mice, thus closely associating CB with emotional behaviours [72]. Importantly, since CB+, PV+ and CR+ neurons constitute the main subsets of GABA+ population which play fairly different roles in the amygdala intrinsic inhibitory system [42,43], any alterations in the activity of these populations

may have a huge impact on this system and inhibitory/excitatory balance. However, it is unclear whether reduced CB expression in the amygdala of the ER β knock-out mice reflects a real reduction in the CB+ cell numbers [73] or a decrease in protein expression [74]. The presence of CB deficit in these mice without any changes in PV and SOM markers, which are present in non-overlapping subpopulations comprising a large part of the CB+ population [50], strongly supports the latter hypothesis. Moreover, unchanged expressions of VGAT and GABA $_A$ α 1 (present study), as well as GAD [24] which occurs in the majority of CB+ neurons, strengthens this hypothesis. However, severe neuronal deficits in all main amygdala regions (which contain many CB+ cells) and the existence of CB+ neurons (which do not co-express PV, SOM or GAD) [37,50] do not exclude the former hypothesis. Another important question is whether there is any compensation mechanism of the reduced CB expression. Schwaller [75] claims that neurons, once committed to expressing a particular calcium-binding protein (CaBP), are either incapable of turning on the expression of another EF-hand family member or that the distinct properties of any other CaBP would not suffice to restore “normal” Ca $^{2+}$ homeostasis. On the other hand, Kreiner et al. [76] revealed that a consequence of loss of PV and CB is alterations in Cav2.1 channels. Modification of Cav2.1 properties through molecular switching of α 12.1 splice variants and β subunits may represent a general mechanism for protecting neurons against aberrant Ca $^{2+}$ signalling and pathological Ca $^{2+}$ overloads [76]. Even when such compensation mechanisms exist, they may not be sufficient to protect neurons from abnormal Ca $^{2+}$ signalling. At any rate, there are several mechanisms by which CB downregulation (even without an actual loss of CB+ neurons) may influence GABAergic inhibition. For example, a CB deficit would be expected to reduce interneuron firing [69] since downregulation of this protein renders the neuron in a less excitable state [70], probably due to the decreased capability to buffer transient intracellular Ca $^{2+}$, which probably changes the duration of depolarisation and, perhaps more significantly, changes repolarisation events [71]. Persistent firing in such a situation may lead to a resting state in these neurons and will subsequently disinhibit the output of the pyramidal neurons [71]. One more mechanism concerning the CB reduction in ER β knock-out mice is worth discussing. According to Schwaller [77], the absence of CB in neurons does not affect basal synaptic transmission but enhances facilitation and shortens delayed transmitter release [78,79]. Such a phenomenon is called “pseudofacilitation” because the main effect of CB leads to an amplitude decrease in inhibitory postsynaptic potential [77]. Interestingly, studies of CB knock-out mice revealed that animals of both sexes show less anxiety, indicating that CB lowering may have anxiolytic effects and may be a compensatory mechanism for maintaining GABAergic neurotransmission at a sufficient level [72].

The study also shows that the expressions of GABA $_A$ α 1 receptor and VGAT were unchanged in ER β knock-out female mice when tested by immunohistochemistry. Unchanged content of the expression of benzodiazepine-sensitive GABA $_A$ receptors in these mice was also previously reported [24]. The expression of α 1 subunit of GABA $_A$ receptor also did not change in the amygdala of high anxiety-related behaviour (HAB) mice compared with matched control, although the content of other subunits (such as α 5, β 1, β 2, γ 1 and γ 2) was altered in these mice [80]. Interestingly, GAD expression was unchanged in ER β knock-out mice [24], while in HAB mice it increased [80], suggesting that the mechanism of increased anxiety is different in both these cases. The unchanged content of VGAT reported in the present study was also observed in the amygdala of helpless rats, one of the animal models of depression [81] and stressed aged mice [82].

ER β knock-out mice have a significantly reduced number of neurons in all amygdala nuclei. Moreover, in the selected amygdala regions, such as ME, BM and CO, neuronal deficits are accompanied by astrocyte overexpression, which is not observed in other amygdala regions. The severity of neuronal deficits and astrocyte overexpression seems to coincide with ER β distribution within the amygdala since ME, BM and CO are especially rich in ER β in wild-type animals [50,83,84]. The present data are thus consistent with the studies of Wang et al. [27], who reported severe neuronal deficits and astroglia overex-

pression in ME of ER β knock-out mice. A similar phenomenon was also reported in the amygdala as well as the hippocampus and prefrontal cortex of ovariectomised rats [51,85] under conditions similar to those in postmenopausal women. Interestingly, in these rats, GABA transporter type 3 (GAT3) was also overexpressed in the amygdala [51]. Since GAT3 is mainly synthesised in astrocytes [86] and GABA concentration in the synaptic gap is heavily controlled by glial cells [87], GAT3 overexpression may result in excessive uptake of GABA and reduced GABA availability in the synaptic cleft [86]. Thus, increased astroglia overexpression could impair overall GABA performance, resulting in the inhibitory/excitatory alteration and emotional disturbances observed in ovariectomised rats [51]. However, it seems that this is not the case in ER β knock-out female mice since astrocyte overexpression is not present in LA, BL and CE, which are essential for fear processing [87]. Although the exact mechanism of neuronal deficits after ER β knock-out is still unknown, there are several explanations. For example, ER β is critically involved during brain development, and its disruption may promote the excessive death of neurons and/or incorrect neuronal migration in this period [88,89], which may partially explain neuronal deficits in quite young mice aged 8–10 weeks, as in the present results and Wang's [27]. However, neuronal deficits increase with age [27], suggesting that there is also another mechanism after this period. Indeed, ER β acts as a key element in neuron lifespan, and its disruption may lead to increased neuronal death [90]. The global disruption of ER β may impair neuroprotective mechanisms and force neurons to die, which results in the neuronal deficits observed in the present study. It is noteworthy that neuronal deficits are also not restricted to the amygdala but are global since severe neuronal deficit in these mice was reported in the cortex, hypothalamus, ventral tegmental area, dorsal raphe nucleus and locus coeruleus; however, they were not present in the caudate-putamen, thalamus and hippocampus [27].

One more issue is worth discussing—i.e., what the clinical implications of the present results are. These results provide evidence that the expression of CB, a marker of the largest subset of GABA $^{+}$ neurons [37], in the amygdala of ER β knock-out female mice is significantly reduced as compared with ER $\beta^{+/+}$. Furthermore, in these mice there are severe cellular deficits in all regions of the amygdala, which increase with age [27]. Thus, in addition to ER β [90], CB may be another potential therapeutic target that may help treat mood disorders in people with decreased oestrogen signalling, including menopausal women [51]. Interestingly, CB expression is decreased in ovariectomised rats, a state in which oestrogen levels are similar to those of menopausal women [51]. This view may be supported by the following facts. Alterations in CB content influence fear and anxiety in mice, evidencing that this protein is closely linked with emotional behaviours [72]. Furthermore, oestrogens have a direct effect on the transcription of the CB gene [91] via oestrogen-responsive elements in the CB promoter [91]. Thus, some effects of oestrogen therapy may be due to CB-promoting pathways. Finally, treatment with vitamin D in rats after ovariectomy increased CB levels, accompanied by a reduction in apoptosis, neuronal damage and depression-like behaviour [83]. Thus, the latter study indicates that clinical actions through CB-promoting pathways may also help prevent to some extent neurodegeneration in subjects with reduced ER β signalling. As CB is involved in various psychiatric disorders [27,69,92–95], clinical actions through CB-promoting pathways may represent a new strategy for preventing and/or treating neurological diseases in women.

In conclusion, these data provide evidence that the density of CB $^{+}$ neurons, the largest subset of GABAergic interneurons [37] in the amygdala of ER β knock-out female mice, was significantly reduced as compared with matched controls, while the other markers of the GABAergic system remained unchanged. In addition, in these mice, there are severe neuronal deficits in all main amygdala regions, which are accompanied by astroglia overexpression in ME, BM and CO. Thus, it appears that the lack of ER β in mutant female mice affects CB expression of GABAergic neurons, causing a reduction in interneuron firing [69] and, finally, a disinhibitory effect over pyramidal function [71]. This fear-promoting excitatory/inhibitory alteration may lead to the increased anxiety observed in

these mice. The impact of neuronal deficits and astroglia overexpression on the amygdala functions is still unknown.

Author Contributions: Conceptualization, D.K. and M.R.; data curation, D.K.; formal analysis, D.K., K.B.-N., A.K. and M.R.; funding acquisition, M.R.; investigation, D.K.; methodology, D.K. and K.B.-N.; project administration, M.R.; supervision, K.B.-N. and M.R.; writing—original draft, D.K.; writing—review and editing, D.K., K.B.-N., A.K. and M.R. All authors have read and agreed to the published version of the manuscript.

Funding: This research was funded by the Faculty of Biology and Biotechnology, University of Warmia and Mazury in Olsztyn, Poland, statutory grant number 12.610.001-300.

Informed Consent Statement: Not applicable.

Data Availability Statement: The data that support the findings of this study are available from the corresponding author upon reasonable request.

Conflicts of Interest: The authors declare no conflict of interest.

References

1. Kessler, R.C.; Angermeyer, M.; Anthony, J.C.; DE Graaf, R.; Demyttenaere, K.; Gasquet, I.; DE Girolamo, G.; Gluzman, S.; Gureje, O.; Haro, J.M.; et al. Lifetime Prevalence and Age-of-Onset Distributions of Mental Disorders in the World Health Organization's World Mental Health Survey Initiative. *World Psychiatry* **2007**, *6*, 168–176. [PubMed]
2. Steel, Z.; Marnane, C.; Iranpour, C.; Chey, T.; Jackson, J.W.; Patel, V.; Silove, D. The Global Prevalence of Common Mental Disorders: A Systematic Review and Meta-Analysis 1980–2013. *Int. J. Epidemiol.* **2014**, *43*, 476–493. [CrossRef] [PubMed]
3. Craske, M.G.; Stein, M.B. Anxiety. *Lancet* **2016**, *388*, 3048–3059. [CrossRef]
4. Nomura, M.; Durbak, L.; Chan, J.; Smithies, O.; Gustafsson, J.-Å.; Korach, K.S.; Pfaff, D.W.; Ogawa, S. Genotype/Age Interactions on Aggressive Behavior in Gonadally Intact Estrogen Receptor β Knockout (BERKO) Male Mice. *Horm. Behav.* **2002**, *41*, 288–296. [CrossRef] [PubMed]
5. Baxter, A.J.; Scott, K.M.; Vos, T.; Whiteford, H.A. Global Prevalence of Anxiety Disorders: A Systematic Review and Meta-Regression. *Psychol. Med.* **2013**, *43*, 897–910. [CrossRef] [PubMed]
6. Bandelow, B.; Michaelis, S. Epidemiology of Anxiety Disorders in the 21st Century. *Dialogues Clin. Neurosci.* **2015**, *17*, 327–335.
7. Ritchie, H.; Roser, M. Mental Health. Our World Data. 2018. Available online: <https://ourworldindata.org/mental-health> (accessed on 17 March 2021).
8. Locke, A.; Kirst, N.; Shultz, C.G. Diagnosis and Management of Generalized Anxiety Disorder and Panic Disorder in Adults. *AFP* **2015**, *91*, 617–624.
9. LeDoux, J. The Emotional Brain, Fear, and the Amygdala. *Cell. Mol. Neurobiol.* **2003**, *23*, 727–738. [CrossRef] [PubMed]
10. Etkin, A.; Prater, K.E.; Schatzberg, A.F.; Menon, V.; Greicius, M.D. Disrupted Amygdalar Subregion Functional Connectivity and Evidence of a Compensatory Network in Generalized Anxiety Disorder. *Arch. Gen. Psychiatry* **2009**, *66*, 1361–1372. [CrossRef]
11. Ramasubbu, R.; Konduru, N.; Cortese, F.; Bray, S.; Gaxiola, I.; Goodyear, B. Reduced Intrinsic Connectivity of Amygdala in Adults with Major Depressive Disorder. *Front. Psychiatry* **2014**, *5*, 17. [CrossRef]
12. Cullen, K.R.; Vizueta, N.; Thomas, K.M.; Han, G.J.; Lim, K.O.; Camchong, J.; Mueller, B.A.; Bell, C.H.; Heller, M.D.; Schulz, S.C. Amygdala Functional Connectivity in Young Women with Borderline Personality Disorder. *Brain Connect.* **2011**, *1*, 61. [CrossRef]
13. Buffalari, D.M.; See, R.E. Amygdala Mechanisms of Pavlovian Psychostimulant Conditioning and Relapse. *Curr. Top. Behav. Neurosci.* **2010**, *3*, 73–99. [CrossRef]
14. Swaab, D.F.; Chung, W.C.J.; Kruijver, F.P.M.; Hofman, M.A.; Hestiantoro, A. Sex Differences in the Hypothalamus in the Different Stages of Human Life. *Neurobiol. Aging* **2003**, *24* (Suppl. 1), S1–S16; discussion S17–S19. [CrossRef]
15. Riecher-Rössler, A. Prospects for the Classification of Mental Disorders in Women. *Eur. Psychiatry* **2010**, *25*, 189–196. [CrossRef] [PubMed]
16. Dalal, P.K.; Agarwal, M. Postmenopausal Syndrome. *Indian J. Psychiatry* **2015**, *57*, S222–S232. [CrossRef] [PubMed]
17. Marsh, W.K.; Bromberger, J.T.; Crawford, S.L.; Leung, K.; Kravitz, H.M.; Randolph, J.F.; Joffe, H.; Soares, C.N. Lifelong Estradiol Exposure and Risk of Depressive Symptoms during the Transition to Menopause and Postmenopause. *Menopause* **2017**, *24*, 1351–1359. [CrossRef] [PubMed]
18. Joffe, H.; Cohen, L.S. Estrogen, Serotonin, and Mood Disturbance: Where Is the Therapeutic Bridge? *Biol. Psychiatry* **1998**, *44*, 798–811. [CrossRef]
19. O'Bryant, S.E.; Palav, A.; McCaffrey, R.J. A Review of Symptoms Commonly Associated with Menopause: Implications for Clinical Neuropsychologists and Other Health Care Providers. *Neuropsychol. Rev.* **2003**, *13*, 145–152. [CrossRef] [PubMed]
20. Soares, C.N.; Almeida, O.P.; Joffe, H.; Cohen, L.S. Efficacy of Estradiol for the Treatment of Depressive Disorders in Perimenopausal Women: A Double-Blind, Randomized, Placebo-Controlled Trial. *Arch. Gen. Psychiatry* **2001**, *58*, 529–534. [CrossRef]

21. Bromberger, J.T.; Kravitz, H.M.; Chang, Y.; Randolph, J.F.; Avis, N.E.; Gold, E.B.; Matthews, K.A. Does Risk for Anxiety Increase during the Menopausal Transition? Study of Women's Health Across the Nation. *Menopause J. N. Am. Menopause Soc.* **2013**, *20*, 488. [\[CrossRef\]](#)
22. Hoyt, L.T.; Falconi, A. Puberty and Perimenopause: Reproductive Transitions and Their Implications for Women's Health. *Soc. Sci. Med.* **2015**, *132*, 103–112. [\[CrossRef\]](#)
23. Gupta, R.R.; Sen, S.; Diepenhorst, L.L.; Rudick, C.N.; Maren, S. Estrogen Modulates Sexually Dimorphic Contextual Fear Conditioning and Hippocampal Long-Term Potentiation (LTP) in Rats(1). *Brain Res.* **2001**, *888*, 356–365. [\[CrossRef\]](#)
24. Krężel, W.; Dupont, S.; Krust, A.; Chambon, P.; Chapman, P.F. Increased Anxiety and Synaptic Plasticity in Estrogen Receptor β -Deficient Mice. *Proc. Natl. Acad. Sci. USA* **2001**, *98*, 12278–12282. [\[CrossRef\]](#) [\[PubMed\]](#)
25. Lund, T.D.; Rovis, T.; Chung, W.C.J.; Handa, R.J. Novel Actions of Estrogen Receptor- β on Anxiety-Related Behaviors. *Endocrinology* **2005**, *146*, 797–807. [\[CrossRef\]](#)
26. Oyola, M.G.; Portillo, W.; Reyna, A.; Foradori, C.D.; Kudwa, A.; Hinds, L.; Handa, R.J.; Mani, S.K. Anxiolytic Effects and Neuroanatomical Targets of Estrogen Receptor- β (ER β) Activation by a Selective ER β Agonist in Female Mice. *Endocrinology* **2012**, *153*, 837–846. [\[CrossRef\]](#) [\[PubMed\]](#)
27. Wang, L.; Andersson, S.; Warner, M.; Gustafsson, J.-A. Morphological Abnormalities in the Brains of Estrogen Receptor Knockout Mice. *Proc. Natl. Acad. Sci. USA* **2001**, *98*, 2792–2796. [\[CrossRef\]](#) [\[PubMed\]](#)
28. Li, X.; Wang, Z.; Tan, L.; Wang, Y.; Lu, C.; Chen, R.; Zhang, S.; Gao, Y.; Liu, Y.; Yin, Y.; et al. Correcting MiR92a-VGAT-Mediated GABAergic Dysfunctions Rescues Human Tau-Induced Anxiety in Mice. *Mol. Ther.* **2017**, *25*, 140–152. [\[CrossRef\]](#) [\[PubMed\]](#)
29. Koyama, S.; Kubo, C.; Rhee, J.-S.; Akaike, N. Presynaptic Serotonergic Inhibition of GABAergic Synaptic Transmission in Mechanically Dissociated Rat Basolateral Amygdala Neurons. *J. Physiol.* **1999**, *518*, 525–538. [\[CrossRef\]](#)
30. Sibille, E.; Pavlides, C.; Benke, D.; Toth, M. Genetic Inactivation of the Serotonin $1A$ Receptor in Mice Results in Downregulation of Major GABA A Receptor α Subunits, Reduction of GABA A Receptor Binding, and Benzodiazepine-Resistant Anxiety. *J. Neurosci.* **2000**, *20*, 2758–2765. [\[CrossRef\]](#)
31. Stutzmann, G.E.; LeDoux, J.E. GABAergic Antagonists Block the Inhibitory Effects of Serotonin in the Lateral Amygdala: A Mechanism for Modulation of Sensory Inputs Related to Fear Conditioning. *J. Neurosci.* **1999**, *19*, RC8. [\[CrossRef\]](#) [\[PubMed\]](#)
32. Gundlach, C.; Pecins-Thompson, M.; Schutzer, W.E.; Bethea, C.L. Ovarian Steroid Effects on Serotonin $1A$, $2A$ and $2C$ Receptor mRNA in Macaque Hypothalamus. *Mol. Brain Res.* **1999**, *63*, 325–339. [\[CrossRef\]](#)
33. Osterlund, M.K.; Halldin, C.; Hurd, Y.L. Effects of Chronic 17β -Estradiol Treatment on the Serotonin 5-HT(1A) Receptor mRNA and Binding Levels in the Rat Brain. *Synapse* **2000**, *35*, 39–44. [\[CrossRef\]](#)
34. Pitkänen, A.; Amaral, D.G. The Distribution of GABAergic Cells, Fibers, and Terminals in the Monkey Amygdaloid Complex: An Immunohistochemical and in Situ Hybridization Study. *J. Neurosci.* **1994**, *14*, 2200–2224. [\[CrossRef\]](#) [\[PubMed\]](#)
35. Capogna, M. GABAergic Cell Type Diversity in the Basolateral Amygdala. *Curr. Opin. Neurobiol.* **2014**, *26*, 110–116. [\[CrossRef\]](#)
36. Prager, E.M.; Bergstrom, H.C.; Wynn, G.H.; Braga, M.F.M. The Basolateral Amygdala GABAergic System in Health and Disease. *J. Neurosci. Res.* **2016**, *94*, 548–567. [\[CrossRef\]](#)
37. Kempainen, S.; Pitkänen, A. Distribution of Parvalbumin, Calretinin, and Calbindin-D(28k) Immunoreactivity in the Rat Amygdaloid Complex and Colocalization with Gamma-Aminobutyric Acid. *J. Comp. Neurol.* **2000**, *426*, 441–467. [\[CrossRef\]](#)
38. McDonald, A.J.; Mascagni, F. Colocalization of Calcium-Binding Proteins and GABA in Neurons of the Rat Basolateral Amygdala. *Neuroscience* **2001**, *105*, 681–693. [\[CrossRef\]](#)
39. Mascagni, F.; Muly, E.C.; Rainnie, D.G.; McDonald, A.J. Immunohistochemical Characterization of Parvalbumin-Containing Interneurons in the Monkey Basolateral Amygdala. *Neuroscience* **2009**, *158*, 1541–1550. [\[CrossRef\]](#)
40. Sorvari, H.; Soininen, H.; Paljärvi, L.; Karkola, K.; Pitkänen, A. Distribution of Parvalbumin-Immunoreactive Cells and Fibers in the Human Amygdaloid Complex. *J. Comp. Neurol.* **1995**, *360*, 185–212. [\[CrossRef\]](#) [\[PubMed\]](#)
41. Sorvari, H.; Miettinen, R.; Soininen, H.; Pitkänen, A. Parvalbumin-Immunoreactive Neurons Make Inhibitory Synapses on Pyramidal Cells in the Human Amygdala: A Light and Electron Microscopic Study. *Neurosci. Lett.* **1996**, *217*, 93–96. [\[CrossRef\]](#)
42. Woodruff, A.R.; Sah, P. Inhibition and Synchronization of Basal Amygdala Principal Neuron Spiking by Parvalbumin-Positive Interneurons. *J. Neurophysiol.* **2007**, *98*, 2956–2961. [\[CrossRef\]](#)
43. Muller, J.F.; Mascagni, F.; McDonald, A.J. Postsynaptic Targets of Somatostatin-Containing Interneurons in the Rat Basolateral Amygdala. *J. Comp. Neurol.* **2007**, *500*, 513–529. [\[CrossRef\]](#)
44. Gulyás, A.I.; Hájos, N.; Freund, T.F. Interneurons Containing Calretinin Are Specialized to Control Other Interneurons in the Rat Hippocampus. *J. Neurosci.* **1996**, *16*, 3397–3411. [\[CrossRef\]](#)
45. Melchitzky, D.S.; Lewis, D.A. Dendritic-Targeting GABA Neurons in Monkey Prefrontal Cortex: Comparison of Somatostatin- and Calretinin-Immunoreactive Axon Terminals. *Synapse* **2008**, *62*, 456–465. [\[CrossRef\]](#)
46. Meskenaite, V. Calretinin-Immunoreactive Local Circuit Neurons in Area 17 of the Cynomolgus Monkey, *Macaca Fascicularis*. *J. Comp. Neurol.* **1997**, *379*, 113–132. [\[CrossRef\]](#)
47. Gonchar, Y.; Burkhalter, A. Connectivity of GABAergic Calretinin-Immunoreactive Neurons in Rat Primary Visual Cortex. *Cereb. Cortex* **1999**, *9*, 683–696. [\[CrossRef\]](#) [\[PubMed\]](#)
48. Kritzer, M.F. Regional, Laminar and Cellular Distribution of Immunoreactivity for ER in the Cerebral Cortex of Hormonally Intact, Postnatally Developing Male and Female Rats. *Cereb. Cortex* **2005**, *16*, 1181–1192. [\[CrossRef\]](#) [\[PubMed\]](#)

49. Równiak, M. The Neurons Expressing Calcium-Binding Proteins in the Amygdala of the Guinea Pig: Precisely Designed Interface for Sex Hormones. *Brain Struct. Funct.* **2017**, *222*, 3775–3793. [[CrossRef](#)] [[PubMed](#)]
50. Fang, Y.-Y.; Zeng, P.; Qu, N.; Ning, L.-N.; Chu, J.; Zhang, T.; Zhou, X.-W.; Tian, Q. Evidence of Altered Depression and Dementia-Related Proteins in the Brains of Young Rats after Ovariectomy. *J. Neurochem.* **2018**, *146*, 703–721. [[CrossRef](#)] [[PubMed](#)]
51. Walf, A.A.; Koonce, C.J.; Frye, C.A. Estradiol or Diarylpropionitrile Decrease Anxiety-like Behavior of Wildtype, but Not Estrogen Receptor Beta Knockout, Mice. *Behav. Neurosci.* **2008**, *122*, 974–981. [[CrossRef](#)] [[PubMed](#)]
52. McDonald, A.J.; Mascagni, F. Immunohistochemical Characterization of Somatostatin Containing Interneurons in the Rat Basolateral Amygdala. *Brain Res.* **2002**, *943*, 237–244. [[CrossRef](#)]
53. Dombret, C.; Naulé, L.; Trouillet, A.-C.; Parmentier, C.; Hardin-Pouzet, H.; Mhaouty-Kodja, S. Effects of Neural Estrogen Receptor Beta Deletion on Social and Mood-Related Behaviors and Underlying Mechanisms in Male Mice. *Sci. Rep.* **2020**, *10*, 6242. [[CrossRef](#)] [[PubMed](#)]
54. Nilsson, M.E.; Vandenput, L.; Tivesten, Å.; Norlén, A.-K.; Lagerquist, M.K.; Windahl, S.H.; Börjesson, A.E.; Farman, H.H.; Poutanen, M.; Benrick, A.; et al. Measurement of a Comprehensive Sex Steroid Profile in Rodent Serum by High-Sensitive Gas Chromatography-Tandem Mass Spectrometry. *Endocrinology* **2015**, *156*, 2492–2502. [[CrossRef](#)] [[PubMed](#)]
55. Równiak, M.; Bogus-Nowakowska, K.; Robak, A. The Densities of Calbindin and Parvalbumin, but Not Calretinin Neurons, Are Sexually Dimorphic in the Amygdala of the Guinea Pig. *Brain Res.* **2015**, *1604*, 84–97. [[CrossRef](#)] [[PubMed](#)]
56. Bentea, E.; Van der Perren, A.; Van Liefferinge, J.; El Arfani, A.; Albertini, G.; Demuyser, T.; Merckx, E.; Michotte, Y.; Smolders, I.; Baekelandt, V.; et al. Nigral Proteasome Inhibition in Mice Leads to Motor and Non-Motor Deficits and Increased Expression of Ser129 Phosphorylated α -Synuclein. *Front. Behav. Neurosci.* **2015**, *9*, 68. [[CrossRef](#)]
57. Du, T.; Chen, Y.; Shi, L.; Liu, D.; Liu, Y.; Yuan, T.; Zhang, X.; Zhu, G.; Zhang, J. Deep Brain Stimulation of the Anterior Nuclei of the Thalamus Relieves Basal Ganglia Dysfunction in Monkeys with Temporal Lobe Epilepsy. *CNS Neurosci. Ther.* **2021**, *27*, 341–351. [[CrossRef](#)]
58. Deng, J.V.; Wan, Y.; Wang, X.; Cohen, S.; Wetsel, W.C.; Greenberg, M.E.; Kenny, P.J.; Calakos, N.; West, A.E. MeCP2 Phosphorylation Limits Psychostimulant-Induced Behavioral and Neuronal Plasticity. *J. Neurosci.* **2014**, *34*, 4519–4527. [[CrossRef](#)]
59. Molgaard, S.; Ulrichsen, M.; Boggild, S.; Holm, M.-L.; Vaegter, C.; Nyengaard, J.; Glerup, S. Immunofluorescent Visualization of Mouse Interneuron Subtypes. *F1000Res* **2014**, *3*, 242. [[CrossRef](#)]
60. Równiak, M.; Kolenkiewicz, M.; Kozłowska, A. Parvalbumin, but Not Calretinin, Neurons Express High Levels of A1-Containing GABAA Receptors, A7-Containing Nicotinic Acetylcholine Receptors and D2-Dopamine Receptors in the Basolateral Amygdala of the Rat. *J. Chem. Neuroanat.* **2017**, *86*, 41–51. [[CrossRef](#)] [[PubMed](#)]
61. Huo, J.; Ren, S.; Gao, P.; Wan, D.; Rong, S.; Li, X.; Liu, S.; Xu, S.; Sun, K.; Guo, B.; et al. ALG13 Participates in Epileptogenesis via Regulation of GABAA Receptors in Mouse Models. *Cell Death Discov.* **2020**, *6*, 87. [[CrossRef](#)] [[PubMed](#)]
62. Zhang, Z.; Jiao, Y.-Y.; Sun, Q.-Q. Developmental Maturation of Excitation and Inhibition Balance in Principal Neurons across Four Layers of Somatosensory Cortex. *Neuroscience* **2011**, *174*, 10–25. [[CrossRef](#)]
63. Paxinos, G.; Franklin, K.B.J. *The Mouse Brain in Stereotaxic Coordinates*; Gulf Professional Publishing: Oxford, UK, 2004; ISBN 978-0-12-547640-9.
64. Sathyanesan, A.; Ogura, T.; Lin, W. Automated Measurement of Nerve Fiber Density Using Line Intensity Scan Analysis. *J. Neurosci. Methods* **2012**, *206*, 165–175. [[CrossRef](#)] [[PubMed](#)]
65. Meijering, E. FeatureJ: A Java Package for Image Feature Extraction. Available online: <https://imagescience.org/meijering/software/featurej/> (accessed on 17 March 2021).
66. McDonald, A.J.; Mascagni, F. Parvalbumin-Containing Interneurons in the Basolateral Amygdala Express High Levels of the β 1 Subunit of the GABAA Receptor. *J. Comp. Neurol.* **2004**, *473*, 137–146. [[CrossRef](#)] [[PubMed](#)]
67. Kaufmann, W.A.; Humpel, C.; Alheid, G.F.; Marksteiner, J. Compartmentation of Alpha 1 and Alpha 2 GABAA Receptor Subunits within Rat Extended Amygdala: Implications for Benzodiazepine Action. *Brain Res.* **2003**, *964*, 91–99. [[CrossRef](#)]
68. Hörtnagl, H.; Tasan, R.O.; Wieselthaler, A.; Kirchmair, E.; Sieghart, W.; Sperk, G. Patterns of mRNA and Protein Expression for 12 GABAA Receptor Subunits in the Mouse Brain. *Neuroscience* **2013**, *236*, 345–372. [[CrossRef](#)] [[PubMed](#)]
69. Eyles, D.W.; McGrath, J.J.; Reynolds, G.P. Neuronal Calcium-Binding Proteins and Schizophrenia. *Schizophr. Res.* **2002**, *57*, 27–34. [[CrossRef](#)]
70. Köhr, G.; Lambert, C.E.; Mody, I. Calbindin-D28K (CaBP) Levels and Calcium Currents in Acutely Dissociated Epileptic Neurons. *Exp. Brain Res.* **1991**, *85*, 543–551. [[CrossRef](#)]
71. Chard, P.S.; Jordan, J.; Marcuccilli, C.J.; Miller, R.J.; Leiden, J.M.; Roos, R.P.; Ghadge, G.D. Regulation of Excitatory Transmission at Hippocampal Synapses by Calbindin D28k. *Proc. Natl. Acad. Sci. USA* **1995**, *92*, 5144–5148. [[CrossRef](#)]
72. Harris, E.P.; Abel, J.M.; Tejada, L.D.; Rissman, E.F. Calbindin Knockout Alters Sex-Specific Regulation of Behavior and Gene Expression in Amygdala and Prefrontal Cortex. *Endocrinology* **2016**, *157*, 1967–1979. [[CrossRef](#)] [[PubMed](#)]
73. Benes, F.M.; Kwok, E.W.; Vincent, S.L.; Todtenkopf, M.S. A Reduction of Nonpyramidal Cells in Sector CA2 of Schizophrenics and Manic Depressives. *Biol. Psychiatry* **1998**, *44*, 88–97. [[CrossRef](#)]
74. Kaalund, S.S.; Riise, J.; Broberg, B.V.; Fabricius, K.; Karlsen, A.S.; Secher, T.; Plath, N.; Pakkenberg, B. Differential Expression of Parvalbumin in Neonatal Phencyclidine-Treated Rats and Socially Isolated Rats. *J. Neurochem.* **2013**, *124*, 548–557. [[CrossRef](#)]
75. Schwaller, B. The Continuing Disappearance of “Pure” Ca^{2+} Buffers. *Cell. Mol. Life Sci.* **2009**, *66*, 275–300. [[CrossRef](#)] [[PubMed](#)]

76. Kreiner, L.; Christel, C.J.; Benveniste, M.; Schwaller, B.; Lee, A. Compensatory Regulation of Cav2.1 Ca²⁺ Channels in Cerebellar Purkinje Neurons Lacking Parvalbumin and Calbindin D-28k. *J. Neurophysiol.* **2010**, *103*, 371–381. [[CrossRef](#)] [[PubMed](#)]
77. Schwaller, B. Emerging Functions of the “Ca²⁺ Buffers” Parvalbumin, Calbindin D-28k and Calretinin in the Brain. In *Handbook of Neurochemistry and Molecular Neurobiology: Neural Protein Metabolism and Function*; Lajtha, A., Banik, N., Eds.; Springer: Boston, MA, USA, 2007; pp. 197–221. ISBN 978-0-387-30379-6.
78. Rozov, A.; Burnashev, N.; Sakmann, B.; Neher, E. Transmitter Release Modulation by Intracellular Ca²⁺ Buffers in Facilitating and Depressing Nerve Terminals of Pyramidal Cells in Layer 2/3 of the Rat Neocortex Indicates a Target Cell-Specific Difference in Presynaptic Calcium Dynamics. *J. Physiol.* **2001**, *531*, 807–826. [[CrossRef](#)] [[PubMed](#)]
79. Błatow, M.; Caputi, A.; Burnashev, N.; Monyer, H.; Rozov, A. Ca²⁺ Buffer Saturation Underlies Paired Pulse Facilitation in Calbindin-D28k-Containing Terminals. *Neuron* **2003**, *38*, 79–88. [[CrossRef](#)]
80. Tasan, R.O.; Bukovac, A.; Peterschmitt, Y.N.; Sartori, S.B.; Landgraf, R.; Singewald, N.; Sperk, G. Altered GABA Transmission in a Mouse Model of Increased Trait Anxiety. *Neuroscience* **2011**, *183*, 71–80. [[CrossRef](#)] [[PubMed](#)]
81. Zink, M.; Vollmayr, B.; Gebicke-Haerter, P.J.; Henn, F.A. Reduced Expression of GABA Transporter GAT3 in Helpless Rats, an Animal Model of Depression. *Neurochem. Res.* **2009**, *34*, 1584–1593. [[CrossRef](#)] [[PubMed](#)]
82. Wang, H.-L.; Sun, Y.-X.; Liu, X.; Wang, H.; Ma, Y.-N.; Su, Y.-A.; Li, J.-T.; Si, T.-M. Adolescent Stress Increases Depression-like Behaviors and Alters the Excitatory-Inhibitory Balance in Aged Mice. *Chin. Med. J.* **2019**, *132*, 1689–1699. [[CrossRef](#)] [[PubMed](#)]
83. Ma, K.; Xu, A.; Cui, S.; Sun, M.-R.; Xue, Y.-C.; Wang, J.-H. Impaired GABA Synthesis, Uptake and Release Are Associated with Depression-like Behaviors Induced by Chronic Mild Stress. *Transl. Psychiatry* **2016**, *6*, e910. [[CrossRef](#)] [[PubMed](#)]
84. Tye, K.M.; Prakash, R.; Kim, S.-Y.; Fenno, L.E.; Grosenick, L.; Zarabi, H.; Thompson, K.R.; Gradinaru, V.; Ramakrishnan, C.; Deisseroth, K. Amygdala Circuitry Mediating Reversible and Bidirectional Control of Anxiety. *Nature* **2011**, *471*, 358–362. [[CrossRef](#)]
85. Zhang, W.; Guo, Y.; Wang, K.; Chen, L.; Jiang, P. Neuroprotective Effects of Vitamin D and 17β-Estradiol against Ovariectomy-Induced Neuroinflammation and Depressive-like State: Role of the AMPK/NF-KB Pathway. *Int. Immunopharmacol.* **2020**, *86*, 106734. [[CrossRef](#)]
86. Gadea, A.; López-Colomé, A.M. Glial Transporters for Glutamate, Glycine, and GABA: II. GABA Transporters. *J. Neurosci. Res.* **2001**, *63*, 461–468. [[CrossRef](#)] [[PubMed](#)]
87. Chazalon, M.; Paredes-Rodríguez, E.; Morin, S.; Martínez, A.; Cristóvão-Ferreira, S.; Vaz, S.; Sebastiao, A.; Panatier, A.; Boué-Grabot, E.; Miguez, C.; et al. GAT-3 Dysfunction Generates Tonic Inhibition in External Globus Pallidus Neurons in Parkinsonian Rodents. *Cell Rep.* **2018**, *23*, 1678–1690. [[CrossRef](#)]
88. Patrone, C.; Andersson, S.; Korhonen, L.; Lindholm, D. Estrogen Receptor-Dependent Regulation of Sensory Neuron Survival in Developing Dorsal Root Ganglion. *Proc. Natl. Acad. Sci. USA* **1999**, *96*, 10905–10910. [[CrossRef](#)]
89. Wang, L.; Andersson, S.; Warner, M.; Gustafsson, J.-A. Estrogen Receptor (ER) Knockout Mice Reveal a Role for ER in Migration of Cortical Neurons in the Developing Brain. *Proc. Natl. Acad. Sci.* **2003**, *100*, 703–708. [[CrossRef](#)] [[PubMed](#)]
90. Vargas, K.G.; Milic, J.; Zaciragic, A.; Wen, K.; Jaspers, L.; Nano, J.; Dhana, K.; Bramer, W.M.; Kraja, B.; van Beeck, E.; et al. The Functions of Estrogen Receptor Beta in the Female Brain: A Systematic Review. *Maturitas* **2016**, *93*, 41–57. [[CrossRef](#)] [[PubMed](#)]
91. Gill, R.K.; Christakos, S. Regulation by Estrogen through the 5'-Flanking Region of the Mouse Calbindin-D28k Gene. *Mol. Endocrinol.* **1995**, *9*, 319–326. [[CrossRef](#)] [[PubMed](#)]
92. Shortall, S.E.; Brown, A.M.; Newton-Mann, E.; Dawe-Lane, E.; Evans, C.; Fowler, M.; King, M.V. Calbindin Deficits May Underlie Dissociable Effects of 5-HT₆ and MGLu7 Antagonists on Glutamate and Cognition in a Dual-Hit Neurodevelopmental Model for Schizophrenia. *Mol. Neurobiol.* **2020**, *57*, 3439–3457. [[CrossRef](#)] [[PubMed](#)]
93. Helmeke, C.; Ovtscharoff, W.; Poeggel, G.; Braun, K. Imbalance of Immunohistochemically Characterized Interneuron Populations in the Adolescent and Adult Rodent Medial Prefrontal Cortex after Repeated Exposure to Neonatal Separation Stress. *Neuroscience* **2008**, *152*, 18–28. [[CrossRef](#)] [[PubMed](#)]
94. Giachino, C.; Canalia, N.; Capone, F.; Fasolo, A.; Alleva, E.; Riva, M.A.; Cirulli, F.; Peretto, P. Maternal Deprivation and Early Handling Affect Density of Calcium Binding Protein-Containing Neurons in Selected Brain Regions and Emotional Behavior in Periadolescent Rats. *Neuroscience* **2007**, *145*, 568–578. [[CrossRef](#)] [[PubMed](#)]
95. Iritani, S.; Kuroki, N.; Ikeda, K.; Kazamatsuri, H. Calbindin Immunoreactivity in the Hippocampal Formation and Neocortex of Schizophrenics. *Prog. Neuropsychopharmacol. Biol. Psychiatry* **1999**, *23*, 409–421. [[CrossRef](#)]